

Characteristics of Charge Traps and Poling Behavior of Poly (Vinylidene Fluoride)

Jeong Won Seo, Kun Sang Ryoo, and Hoo Sung Lee

Department of Chemistry, Sogang University, 1-1 Shinsoodong, Seoul 121, Korea (Received March 6, 1985)

Transient charging and discharging currents as well as space charge limited currents have been measured in biaxially stretched poly(vinylidene fluoride) film under various poling fields and temperatures. At low temperatures and short poling times, the I-V characteristics showed shallow trap behavior. When the current values extrapolated to the infinite time, the I-V characteristics indicate that the distribution of the trap energy levels is uniform or very broad. The abnormal suppression of current at higher poling voltages and the high discharge rate observed also in the same voltage range are attributed to the morphological changes due to dipole reorientation.

Introduction

During the last fifteen years, pyroelectricity and piezoelectricity in polymers have attracted great attention of many chemists, physicists, and engineers.¹⁻²¹ There are only limited numbers of polymers which are known to have pyro- and/or piezo-electric properties.^{6,22-29} Among such polymers, poly(vinylidene fluoride) (PVDF) has been known to have the highest piezoelectric and pyroelectric coefficients.⁶ PVDF films can be made pyro- and piezo-electric by poling, in which the electric dipoles in the polymer are aligned along the direction of the applied electric field. The electric field is applied via the electrodes attached on both sides of the polymer film.

It is understood that the pyro- and piezo-electricity in PVDF films are attributable to the polarization formed during poling.¹⁻⁹ It is also believed that there is a certain relationship between the magnitude of the polarization and charge injection which inevitably occurs during poling.^{6,30-32} In this paper, in an attempt to understand the role of the injected charges in poling, the characteristics of the injected charges were studied by measuring the space charge limited current during poling, and the transient currents, *i.e.* the charge and discharge current after applying and removal of the poling voltage. When the electrodes are shorted via an electrometer after removal of the poling voltage, discharge current can be observed. Discharge current is due to flow of charges released from the traps. It is also called long term discharge current because the processes of trapping and releasing charges are very slow. Lindmayer³⁴ studied the relationship between the discharge current and the distribution of the trap energy levels in SiO and SiO₂ films. According to Lindmayer's calculation, when the traps have a homogeneous energy distribution and the discharge time is not either too short or too long, the discharge current I should decrease linearly with $1/t$. Therefore, plot of $\log I$ vs. $\log t$ should give a straight line of slope -1 . According to Vanderschueren and Linkens,³⁵ who have studied transient charging and discharging currents in various polymers, the two types of currents are mirror images of each other, *i.e.* of the same magnitude and opposite in sign. They concluded that the transient currents are governed by dipolar mechanisms and depend on the measuring temperature very much. In a study of I-V characteristics of single crystalline polyethylene, van Roggen³⁶ have observed reduction in current density above a certain DC voltage. Such a phenomenon was

attributed to the recrystallization of polyethylene. Similar behavior has been found in low pressure polyethylene. However, in high pressure polyethylene, such a current reduction phenomenon has not been observed.

Theoretical

There have been many illuminating studies on the space charge limited current in insulators.³⁷⁻⁴¹ The most important factors which govern the space charge limited currents are the distribution of the trap energy levels and the spatial distribution of traps inside the film. When the applied voltage is low, the current is mainly carried by the thermal charges.³⁷ The concentration of the thermal charges is determined by thermal equilibrium between the Fermi level and the conduction band.³⁷ Under such circumstances, the current I is proportional to the applied voltage, V , *i.e.* Ohm's law holds.³⁷ Therefore, plot of $\log I$ vs. $\log V$ shows a straight line with a slope of unity as shown in Figure 1 (a). The number of charges injected from the electrodes increases with the applied voltage. Above a certain voltage, the injected charges outnumber the thermal charges. From this cross-over voltage V_c , the current I increases with the square of the applied voltage V , *i.e.* the square law holds and a plot of $\log I$ vs. $\log V$ gives a straight line with a slope of two as shown in Figure 1 (b). This is what can be obtained when there is no trap to hold the charges.

However, in polymer films, there are always some traps due to some impurities and structural imperfections.³⁷ There are two kinds of traps: namely a shallow trap the energy level of which is higher than the Fermi level, and a deep trap the energy level of which is lower than the Fermi level. In the presence of such traps, the current-voltage relationship satisfies the Ohm's law until all the traps are filled and the cross-over voltage is higher than it would have been for the trap free case. In the case of shallow traps, the cross-over occurs at V_c , (Figure 1) and the square-law is followed along line c in Figure 1. If the traps are deep, Ohm's law holds until all the traps are filled at V , in Figure 1. Above this trap filled limit, the sample behaves like trap free one, *i.e.* the current level quickly jumps up to the trap free level represented by line b in Figure 1. However, in the case of shallow traps, the trap filled limit is achieved at a higher voltage than in the case of the deep traps. From this point the current increases along lines e and b.

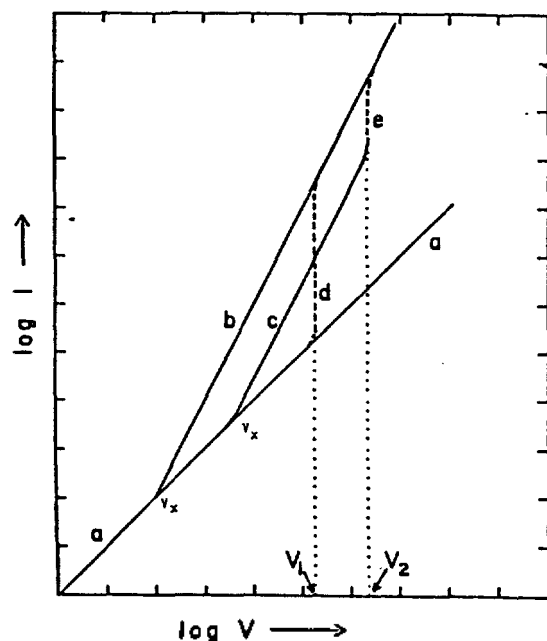


Figure 1. I-V Characteristics of an insulator. a: Ohm's law. b: trap-free square law. c: shallow trap square law. d: trap filled limit with deep traps. e: trap filled limit with shallow traps.

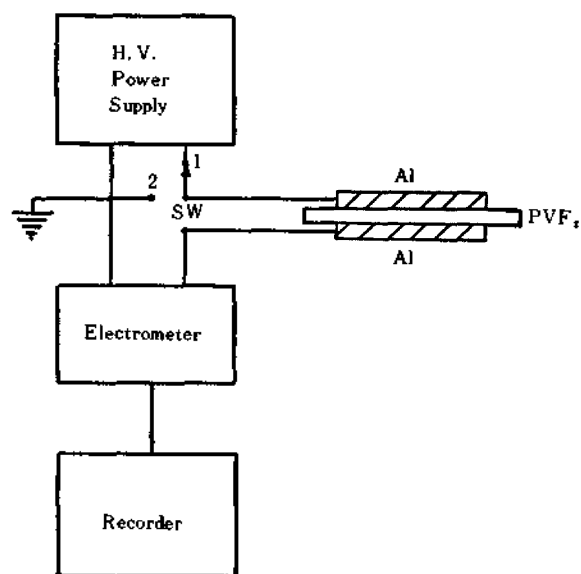


Figure 2. Circuit diagram for poling (SW→1), SCLC measurement (SW→1), and discharging current measurement (SW→2).

When a DC voltage is applied to a piece of polymer film, the current decays monotonically with time. The rate of the decay is very fast in the early stages of poling, then becomes gradually slower as the time elapses. In a relatively short time range, the current can be expressed as a single function of time. However, there is no single function which can represent the current profile satisfactorily in all the time ranges. The following empirical equation, which is often called the Curie-Von Schweidler law, is one of the most frequently used equations:

$$I(t) = A(T)t^{-\alpha} \quad (1)$$

where $I(t)$ is the transient current, $A(T)$ a temperature dependent factor, t the time after application or removal of the DC voltage, and α a constant. Therefore, it is usually necessary to observe the current for a certain period of time.

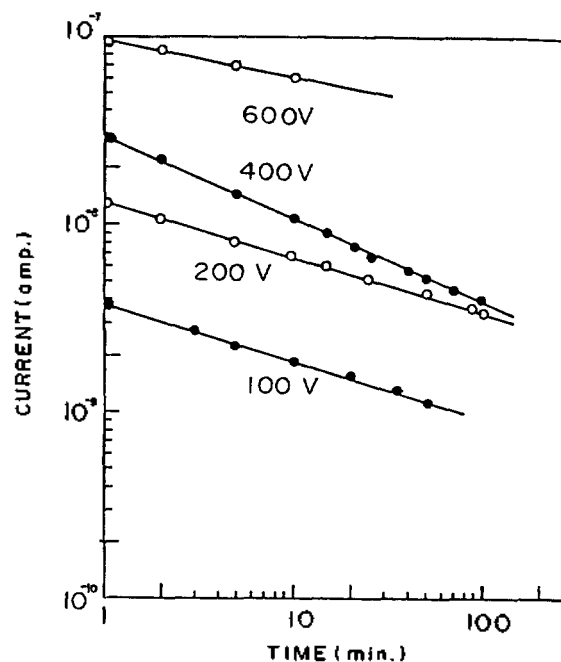


Figure 3. Charging current of PVDF film as a function of time under various applied voltages (room temperature).

Experimental

The PVDF film used in this study was Kureha's biaxially stretched $6 \mu\text{m}$ film. Circular aluminum electrodes were vacuum-evaporated on both sides of the film. The overlapping area of the electrodes were 1 cm^2 . The specimens were heated to the poling temperature and the poling electric field was applied. The circuit used for poling is shown schematically in Figure 2. The current was measured with an electrometer (Kiethly 610C). Measurement of current which was started immediately after the application of the poling field was made as a function of poling time. The discharge current was measured by flipping the switch to position 2 in Figure 2. More details about the experimental procedures are described elsewhere.⁶

Results and Discussion

The charging current is plotted on a double logarithmic scale, in Figure 3, as a function of time. The average α value in equation (1), which was obtained from the slope of the straight lines in Figure 3, was -0.32 ± 0.1 . The current-voltage relationship shown in Figure 4 was obtained with current values measured 20 minutes after application of the poling voltage. As can be seen in Figure 4, the current-voltage relationship, at low temperatures ($<50^\circ\text{C}$) and with short poling times (<20 mins.), shows shallow trap characteristics. The current levels in the regions of both Ohm's law and the square law increase with temperature. This is an indication that the concentrations of both the thermal charges and the injected charges increase with the temperature. It can also be seen in Figure 4 that at higher poling voltages (for instance >200 volts at 30°C), increase in current is significantly suppressed. Similar phenomena have been observed by Setter⁴² in polyethylene film and by van Roggen³⁶ in polyethylene single crystals. In van Roggen's study,³⁶ the phenomenon was attributed to recrystallization of the polymer.

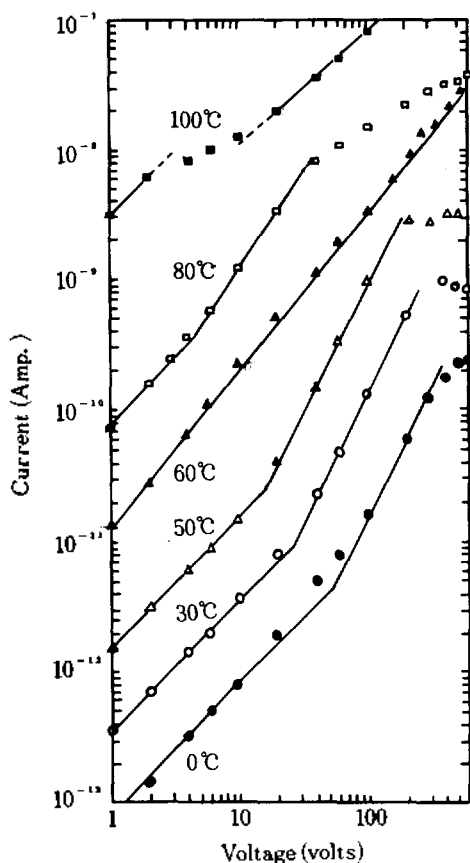


Figure 4. Plot of $\log I$ vs $\log V$ in PVDF film at various temperatures. The currents were measured 20 minutes after the voltage was applied except the data for 60°C which were obtained by extrapolating to $1/t \rightarrow 0$.

In PVDF films, which contains segments with greater dipole moments than in polyethylene, this may be explained as follows: under a high poling voltage, due to the reorientation of the dipoles, the polymer film is expected to experience morphological changes which create more traps to immobilize the charges. More evidence supporting this was found in the measurement of discharge current which will be described later. At high temperatures ($T > 80^\circ\text{C}$) the current was very unpredictable and impossible to analyze by a simple model. Such phenomenon may be explained in terms of acoustic phonon scattering.³⁷ At these higher temperatures, the phenomenon of current suppression was observed at lower voltages. This is rather natural considering that the motions of the polymer chains become facile at higher temperatures.

The current I for 60°C in Figure 4 was obtained by extrapolating the discharge current to $1/t \rightarrow 0$, i.e. to $t \rightarrow \infty$. It is interesting to note that, in Figure 4 at 60°C, no crossover from Ohm's law to the square law was observed. This means that if the discharge current is measured after waiting for infinite period of time, the crossover will not be observed. The slope of the straight line for 60°C was found to be 1.3 which is a value between those for Ohm's law and the square law. It is expected that at $t \rightarrow \infty$, a steady state would be achieved. The fact that the slope of the straight line was 1.3 indicates that the traps do not have a single energy level but a broad distribution of trap energy levels. The result of discharge current measurement also consistent with this.

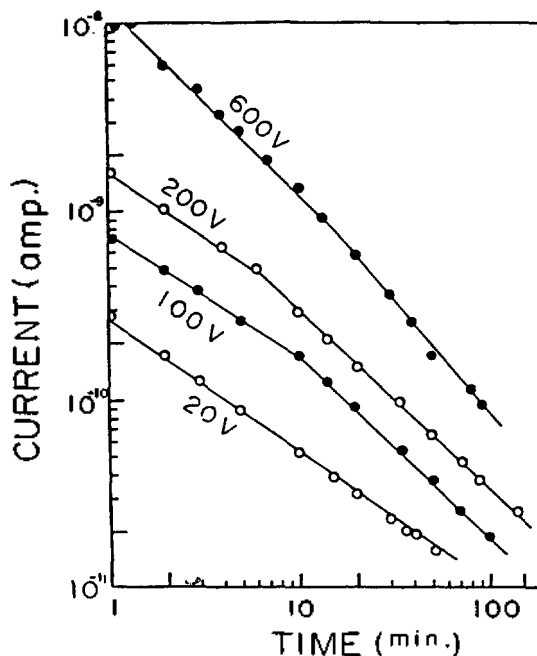


Figure 5. Discharge current of PVDF film after charging at various voltages for 100 minutes (room temperature).

The discharge currents measured with the PVDF specimens for a number of poling (i.e. charging) voltages are plotted in a double logarithmic scale, as a function of time in Figure 5. With low poling voltages (< 20 volts), plot of $\log I$ vs. $\log t$ decreases linearly with a slope of -0.7 , i.e. $\alpha = 0.7$ in equation (1). For intermediate voltages ($20 < V < 200$ volts), in the earlier stages of discharge, the current decreased at the same rate ($\alpha = 0.7$) as for the low poling voltages, then as the discharge time became longer, it decreased at an intermediate rate ($\alpha = 1.0$). For high poling voltages (> 200 volts), in the early stages of discharge, the current decreased at the intermediate rate ($\alpha = 1.0$). Then as the discharge time became longer, it decreased at an even faster rate, i.e. $\alpha = 1.2$. Therefore, at least three distinct slopes have been observed in the above discharge experiments. Since the discharge current is attributable to the release of trapped charges, the characteristics of the discharge current vary with the energy level, the distribution of the energy levels of the traps, and the spatial distribution of traps inside the film. In the measurement of transient currents the Vander-schueren-Linkens³⁵ type symmetry relationship between the charging and discharging currents was not observed in the biaxially stretched PVDF specimens. Moreover, although the Curie-von Schweidler law holds very well for the charging current, more than one α values have been observed in the transient behavior of the discharging current except for the lowest voltage used (20 volts). It is very interesting to note that, with intermediate or high poling voltages, plot of $\log I$ vs. $\log t$ shows a slope of -1 for a certain period of time. This is an indication that, according to Lindmayer,³⁴ the distribution of trap energy levels in this polymer is homogeneous or very broad at least for the intermediate poling voltages, which is a reasonable conclusion for a polymorphous polymer like PVDF.

In the I-V characteristics (Figure 4), at 30°C, the cross-over from the Ohmic behavior to the square-law occurs at about 20 volts. The discharge current showed a single decay rate

($\alpha=0.7$) with a sample poled at 20 volts and two decay rates in the samples poled at above 20 volts ($\alpha=0.7$ and 1.0). Therefore, the PVDF film which has been exposed under a DC voltage less than 20 volts shows a single decay rate of 0.7. On the other hand the PVDF film which has been poled under intermediate voltages shows two different decay rates, namely 0.7 and 1.0. At poling voltages higher than 200 volts (see Figure 4) at 30°C, the I-V characteristics gives the abnormal suppression behavior in the current level. This was attributed to the morphological changes due to dipole reorientation in the polymer film. The discharge current also behaves differently in this voltage range. For instance, for a specimen poled at 600 volts (see Figure 5), the current shows two different decay rates, i.e. $\alpha=1.0$ and 1.2, which are different from those observed at lower voltages. Therefore, PVDF film which has experienced some dipole reorientation, shows the highest decay rate ($\alpha=1.2$) in the longer time range of discharge. It is desirable to study the currents more extensively in conjunction with morphological studies such as the IR spectroscopy and X-ray diffraction techniques.

Acknowledgements. The authors would like to express their thanks to the Korea Research Foundation for the financial support.

References

- (1) H. Kawai, *Japan J. Appl. Phys.*, **8**, 875 (1969).
- (2) K. Nakamura and Wada, *J. Polym. Sci., A-2*, **9**, 161, (1971).
- (3) J. G. Bergman, Jr., J. H. McFee, and G. R. Crane; *Appl. Phys. Lett.*, **18**, (1971).
- (4) A. M. Glass, J. H. McFee, and J. G. Bergman, Jr., *J. Appl. Phys.*, **42**, 5219 (1971).
- (5) T. Furukawa, Y. Uematsu, K. Asakawa, and Y. Wada, *J. Appl. Polym. Sci.*, **12**, 2675 (1968).
- (6) H. Lee, "Pyroelectricity of Homo- and Co-polymeric Vinylidene Fluoride and Blends", Ph.D. Dissertation, Temple University, 1978.
- (7) H. Lee, R. E. Salomon, and M. M. Labes, *Macromolecules*, **11**, 171, (1978).
- (8) D. K. Das-Gupta and K. Doughty, *J. Appl. Phys.*, **11**, 2415 (1978).
- (9) N. Naegele, D. Y. Yoon, and M. G. Broadhurst, *Macromolecules*, **11**, 1297 (1978).
- (10) Dvey-Aharon and P. L. Taylor, *J. Appl. Phys.*, **51**, 5184 (1980).
- (11) N. Takahashi and A. Odajima, *Ferroelectrics*, **32**, 49 (1981).
- (12) S. S. Bamji, K. J. Kao, and M. M. Perlman, *J. Polym. Sci., Polym. Phys. Ed.*, **18**, 1945 (1980).
- (13) N. Takahashi and A. Odajima, *Jap. J. Appl. Phys.*, **20**, L59 (1981).
- (14) M. K. Das-Gupta and K. Doughty, *J. Appl. Phys.*, **49**, 4601 (1978).
- (15) M. Tamura, S. Hgiwara, S. Matsumoto, and N. Ono; *J. Appl. Phys.*, **48**, 513 (1977).
- (16) G. T. Davis, J. E. McKinney, M. G. Broadhurst, and S. C. Roth, *J. Appl. Phys.*, **49**, 4998 (1978).
- (17) J. I. Scheinbeim, K. T. Chung, K. D. Pae, and B. A. Newman, *J. Appl. Phys.*, **51**, 6101 (1979).
- (18) J. I. Scheinbeim, C. H. Yoon, K. D. Pae, and B. A. Newman, *J. Appl. Phys.*, **51**, 5156 (1980).
- (19) T. Furukawa, Date, and G. E. Johnson, *J. Appl. Phys.*, **54**, 1540 (1983).
- (20) B. A. Newman and J. I. Scheinbeim; *Macromolecules*, **16**, 60 (1983).
- (21) P. Cebe and D. T. Grubb, *Macromolecules*, **17**, 1374 (1984).
- (22) K. Tashiro, M. Nakamura, M. Kobayashi, Y. Chatani, and H. Tadokoro; *Macromolecules*, **17**, 1452 (1982).
- (23) T. Yamada; *J. Appl. Phys.*, **53**, 6335 (1982).
- (24) J. McBrierty, D. C. Douglass, and T. Furukawa; *Macromolecules*, **17**, 1136 (1984).
- (25) T. Furukawa, M. Ohuchi, A. Chiba, and M. Date, *Macromolecules*, **17**, 1384 (1984).
- (26) H. Lee, R. E. Salomon, and M. M. Labes, *J. Appl. Phys.*, **50**, 3773 (1979).
- (27) A. I. Baise, H. Lee, B. K. Oh, R. E. Salomon, and M. M. Labes, *Appl. Phys. Lett.*, **26**, 428 (1975).
- (28) M. H. Litt, C. Hsu, and P. Basu, *J. Appl. Phys.*, **48**, 2208 (1977).
- (29) S. Miyata, M. Yoshikawa, S. Tasaka, and M. Ko; *Polymer J.*, **12**, 857 (1980).
- (30) K. Takahashi, H. Lee, R. E. Salomon, and M. M. Labes; *J. Appl. Phys.*, **48**, 4694 (1977).
- (31) N. Murayama, *J. Polym. Sci., Polym. Phys. Ed.*, **13**, 929 (1975).
- (32) N. Murayama and H. Hashizume, *J. Polym. Sci., Polym. Phys. Ed.*, **41**, 989 (1976).
- (33) A. Szymanski, *J. Polym. Sci. Part D., Macromolecular Rev.*, **4**, 245 (1966).
- (34) J. Lindmayer, *J. Appl. Phys.*, **36**, 196 (1965).
- (35) J. Vanderschueren and A. Linkens, *J. Appl. Phys.*, **49**, 4195 (1978).
- (36) A. Van Roggen, *Phys. Rev. Lett.*, **9**, 368 (1962).
- (37) M. A. Lampert and P. Mark, "Current Injection in Solids," Academic Press, New York, 1970.
- (38) R. S. Muller, *Solid State Electronics*, **6**, 25, (1962).
- (39) W. Hwang and K. C. Kao; *Solid State Electronics*, **15**, 523 (1972).
- (40) J. s. Bonham, *Aust. J. Chem.*, **31**, 2117 (1978).
- (41) A. Rose; *Phys. Rev.*, **97**, 1538 (1955).
- (42) G. Setter, *Koll. Z. Polymere*, **215**, 112 (1967).